## Supplementary Information

# Direct detection of microRNA in liquid biopsies from single cancer spheroids

Chen Hu,[a] Essam M. Dief,[a] Bram G. Soliman,[a] Sara Romanazzo,[a] Shilpa Rana,[a] Kristopher A. Kilian,[ab] Richard D. Tilley*[ac] and J. Justin Gooding*[a]

[a] School of Chemistry, Australian Centre for NanoMedicine, The University of New South Wales, Sydney, NSW 2052, Australia.

[b] School of Materials Science and Engineering, The University of New South Wales, Sydney, NSW 2052, Australia.

[c] Electron Microscope Unit, Mark Wainwright Analytical Centre, The University of New South Wales, Sydney, NSW 2052, Australia.

* Corresponding authors. Email: r.tilley@unsw.edu.au; justin.gooding@unsw.edu.au.

## Table of contents

# 1 Supplementary figures and tables

## 1.1 Fig. S1 Scheme illustrating the formation of 1 spheroid

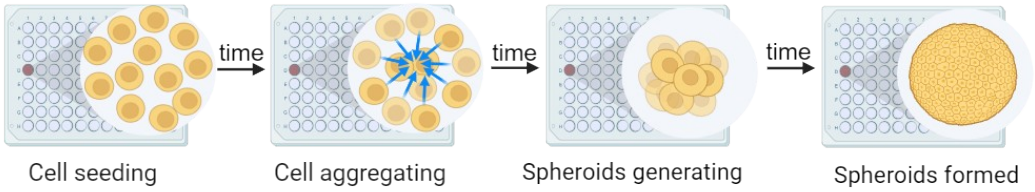


**Fig. S1** Scheme illustrating the formation of 1 spheroid. MCF7 cells were cultured individually for five days in ultra-low attachment plates. At day five, spheroids were transferred to achieve the given numbers of spheroids per well. Spheroids were cultured for two more days in 60 µL media per group. On day seven, media were collected and centrifuged for 5 minutes at 200 G to remove any cellular components.

## 1.2 Fig. S2 TEM characterization and size distribution of the Au@MNPs

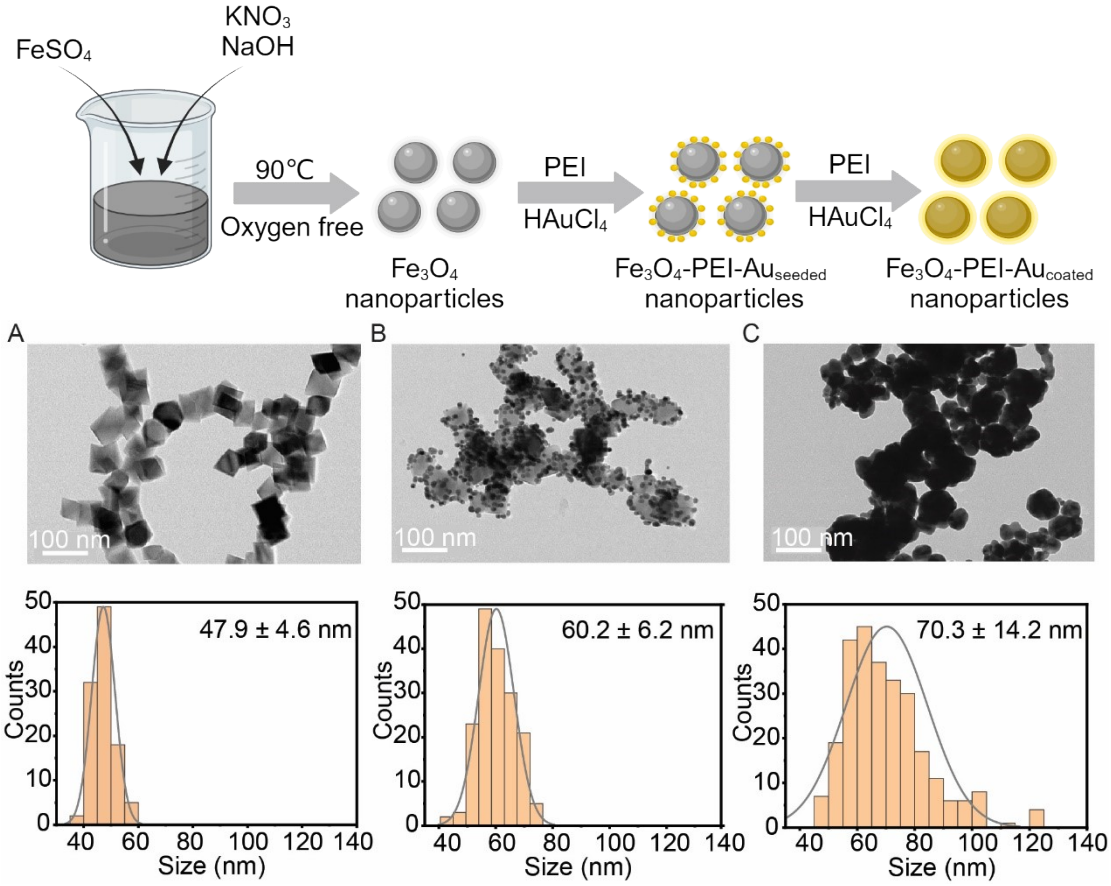


**Fig. S2** Scheme illustrating the synthesis process, TEM characterization and size distribution histograms of the Au@MNPs. (A) The cubic $Fe_3O_4$-PEI nanoparticles are formed with an average size of (47.9±4.6) nm; (B) the core-satellite structure $Fe_3O_4$-PEI-$Au_{seeded}$ nanoparticles are formed with an average size distribution of (60.2±6.2) nm; (C) The gold is further coated to generate the $Fe_3O_4$-PEI-$Au_{coated}$ nanoparticles with the size increased to (70.3±14.2) nm. The scale bar of the TEM images is 100 nm. Image J software was used for calculating the size distribution. These results demonstrated the success of the design of fabricating core-satellite structure and controllable growth of satellite particles through a complete gold coating on magnetic nanoparticles. Detailed characterization on the nanoparticles has been done in our group before[1–5], and summarized below in Table S1.

### 1.3 Table S1 Characterization of the Au@MNPs

**Table S1.** Characterization of Au@MNPs

| **Characterization** | **Reference** |
|---|---|
| UV-vis spectra of the Au@MNPs | 1 |
| Dynamic light scattering (DLS) measurement before and after PEI coating | 1 |
| Scanning electron microscope (SEM) of the Au@MNPs deposited on electrode surface | 3, 5 |
| Atomic force microscopy (AFM) of the Au@MNPs deposited on electrode surface | 5 |
| X-ray photoelectron spectroscopy (XPS) of the Au@MNPs | 1 |
| X-ray photoelectron spectroscopy (XPS) of the Au@MNPs after modification | 2, 3, 4 |
| Aggregation stability of the Au@MNPs | 1 |

### 1.4 Fig. S3 The mechanism of the “dispersible electrodes” sensing platform

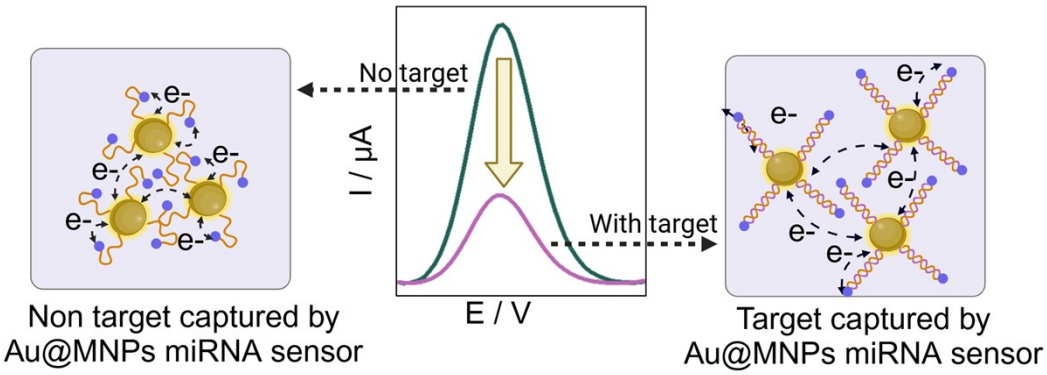


**Fig. S3** The mechanism of the “dispersible electrodes sensing platform”. Once the target miRNA is hybridized onto the Au@MNPs, the formation of DNA-miRNA duplex leads the methylene blue far away from the nanoparticle surfaces, decreasing the electrochemical electron transfer rate constants. The decrease in the square-wave voltammetry peak current is proportional to the target miRNA concentration. Measurements were done in the range between -0.45 V to 0 V (verse Ag|AgCl 3M) with pulse amplitude of 25 mV and frequency of 10 Hz.

## 1.5 Fig. S4 The calibration curve in the buffer

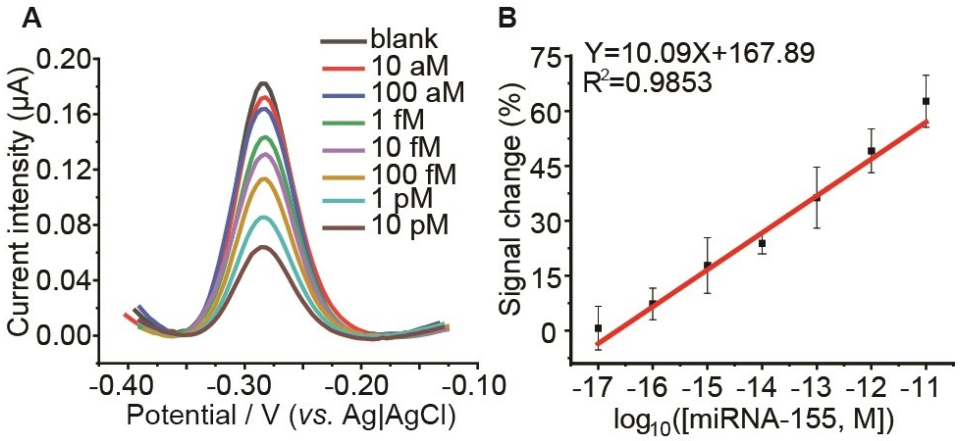


**Fig. S4** The detection ability of the proposed sensor in phosphate-buffered saline solution solution. (A) The current intensity in the square wave voltammograms for the detection of different amounts of miRNA-155 in buffer solution. (B) Current percentage change for different amounts of miRNA-155. Electrolyte: 1× PBS buffer (pH 7.4); frequency: 10 Hz; pulse amplitude: 25 mV. The results show that the relationship between the miRNA-155 to its square wave current in buffer follows a linear correlation equation of Y=10.09X+167.89 ($R^2$=0.9853) and that as low as 10 aM miRNA-155 can be detected in buffered solution.

## 1.6 Fig. S5 Scheme illustrating the procedure for comparing PCR and sensor results on 96 spheroids

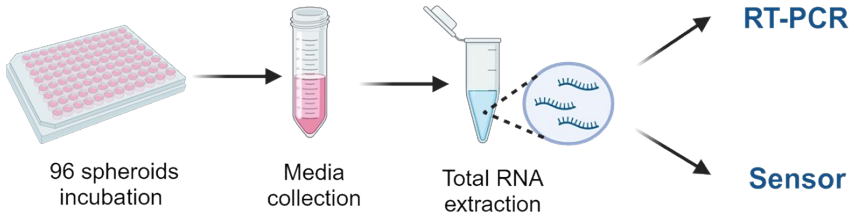


**Fig. S5** Schematic illustration of the procedure for PCR and sensor comparison on 96 spheroids. A plate of 96 spheroids was cultured for 5 days, after which media was collected. The total RNA was extracted from the media and miRNA-155 was measured from the total RNA using both RT-PCR and sensor measurement.

## 1.7 Fig. S6 PCR quantification of miRNA-155 in RNA extracted from the media of 96 spheroids

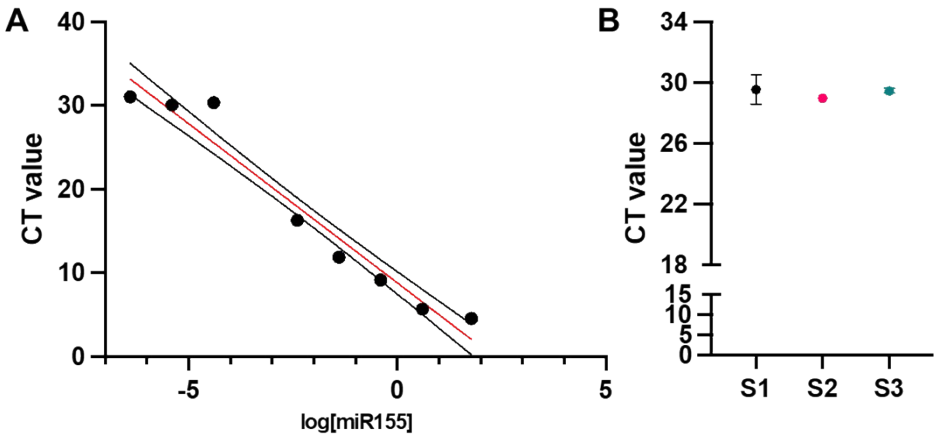


**Fig. S6** (A) Calibration curve of miRNA-155 mimic generated by Ct values obtained by qRT-PCR of serial dilutions of the mimic cDNA. (B) Ct values obtained by qRT-PCR of miRNA-155 in total RNA extracted from 3 samples. Each sample corresponds to media collected from 96 spheroids.

### 1.8 Calculation of miRNA-155 by RT-PCR (for 96 spheroids)

| | Sample 1 | Sample 2 | Sample 3 | Average |
|---|---|---|---|---|
| miRNA-155 (pM) | 4.0±2 | 5.1±1 | 4.0±0.4 | 4.3±1 |

**Table S2.** miRNA-155 released from 96 individually cultured spheroids by PCR

### 1.9 Calculation of miRNA-155 by Au@MNPs miRNA sensor (for 96 spheroids)

**Table S3.** miRNA-155 released from 96 individually cultured spheroids by sensor

| | Sample 1 | Sample 2 | Sample 3 | Average |
|---|---|---|---|---|
| Signal decrease % | 52±12 | 52± 17 | 55± 14 | 49±15 |

By using the calibration curve constructed in the media(Y=10.09X+167.89), miRNA concentration was calculated and the average of miRNA-155 concentration in 96 spheroids is calculated to be 5.6±2 pM.

### 1.10 Fig. S7 Scheme illustrating the generation of 12 spheroids

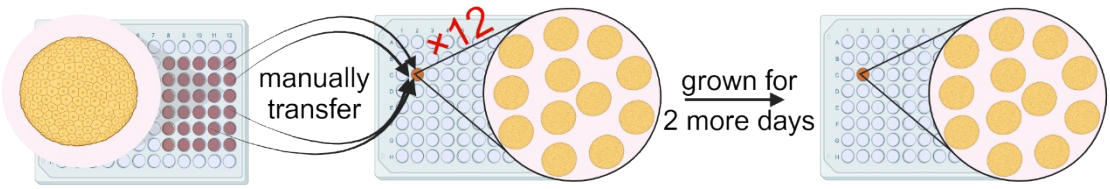


**Fig. S7** Scheme illustrating the generation of 12 spheroids. After spheroid generation, spheroids are manually transferred one by one into the same well until the desired number of spheroids are formed. Then, these spheroids were incubated for two more days after which the media was collected.

### 1.11 Fig. S8 Reproducibility within one batch of 1, 2 and 4 spheroids measurement

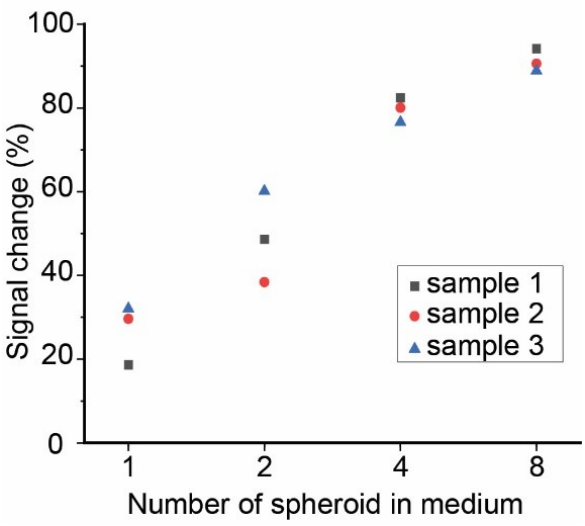


**Fig. S8** Signal change reproducibility among triplicate samples. Electrolyte: 1× PBS buffer (pH 7.4); frequency: 10 Hz; pulse amplitude: 25 mV.

### 1.12 Fig. S9 Result of Batch 2 measurement for 1, 2 and 4 spheroids

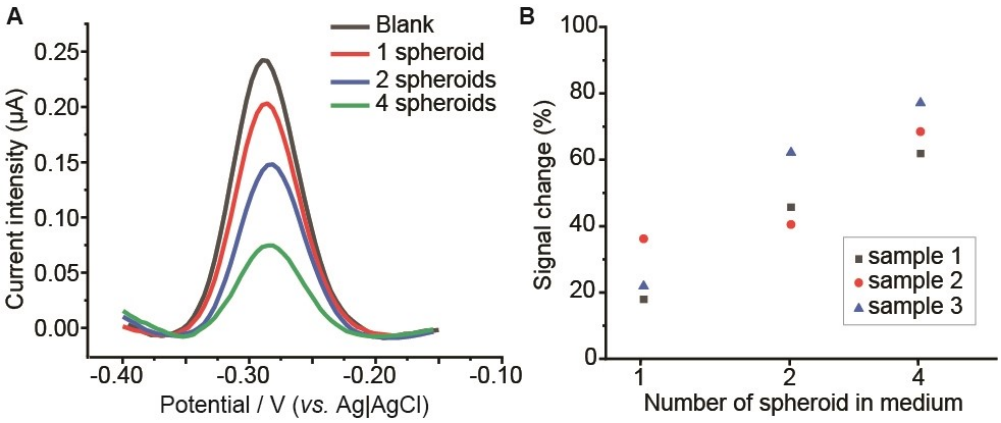


**Fig. S9** Evaluation of the sensor performance with a different batch of cancer spheroids (batch 2). (A) The current intensity in square wave voltammograms for the detection of miRNA-155 in the cell media was obtained from different numbers of spheroids (blank means there are no spheroids but only the media). (B) Signal change reproducibility among triplicate samples for this batch of cancer spheroids. Electrolyte: 1× PBS buffer (pH 7.4); frequency: 10 Hz; pulse amplitude: 25 mV.

### 1.13 Fig. S10 Result of Batch 3 measurement for 1, 2 and 4 spheroids

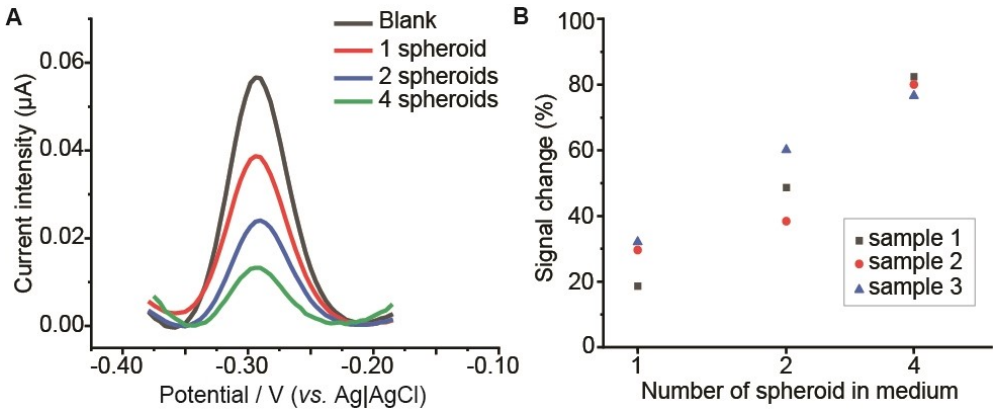


**Fig. S10** Evaluation of the sensor performance with a different batch of cancer spheroids (batch 3). (A) The current intensity in square wave voltammograms for the detection of miRNA-155 in the cell media was obtained from different numbers of spheroids (blank means there are no spheroids but only the media). (B) Signal change reproducibility among triplicate samples for this batch of cancer spheroids. Electrolyte: 1× PBS buffer (pH 7.4); frequency: 10 Hz; pulse amplitude: 25 mV.

## 1.14 Fig. S11 Scheme illustrating the procedure for PCR and sensor measurement

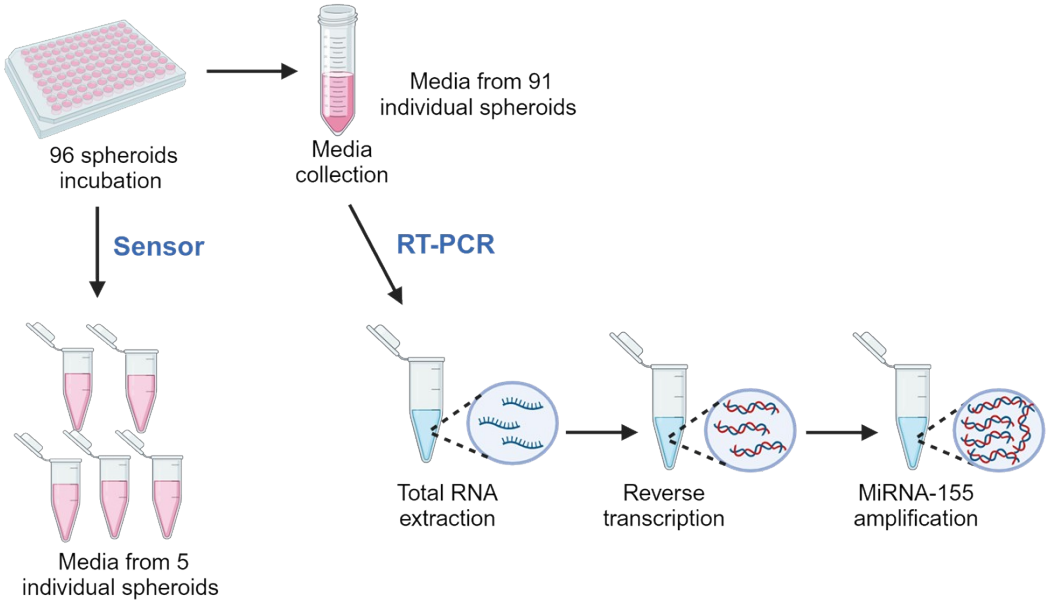


**Fig. S11** Schematic illustration of the procedure for PCR and sensor measurement on the same plate of spheroids. 96 spheroids were cultured individually in wells of a 96-well plate. After the spheroids was grown for eight days, media from five spheroids were collected individually to run the sensor measurement. The media from the rest of 91 spheroids was collected for PCR measurement, with total RNA extracted and miRNA-155 amplified.

### 1.15 Calculation of miRNA-155 by RT-PCR (for 1 spheroid)

| | Measurement 1 | Measurement 2 | Measurement 3 | Average |
|---|---|---|---|---|
| miRNA-155(pM) in 91 spheroids | 17.5 | 19.9 | 15.0 | 17±2 |
| miRNA-155 (fM) in 1 spheroid | 191.8 | 218.8 | 164.4 | 192 ±27 |

**Table S4.** miRNA-155 released from 1 spheroid by PCR

### 1.16 Calculation of miRNA-155 by sensor (for 1 spheroid)

| | Well 1 | Well 2 | Well 3 | Well 4 | Well 5 | Average |
|---|---|---|---|---|---|---|
| Signal decrease % | 45 ±1 | 48±3 | 42±4 | 50±3 | 30±4 | 43±8 |

**Table S5.** miRNA-155 released from 1 individually cultured spheroid by the sensor

miRNA concentration was calculated by using the calibration curve constructed in the media (Y=9.41X+163.26), and the average of miRNA-155 concentration in 1 spheroid is calculated to be 354±63 fM.

**Reference**


1 I. Y. Goon, L. M. H. Lai, M. Lim, P. Munroe, J. J. Gooding and R. Amal, *Chem. Mater.*, 2009, **21**, 673–681.

2 I. Y. Goon, L. M. H. Lai, M. Lim, R. Amal and J. J. Gooding, *Chem. Commun.*, 2010, **46**, 8821–8823.

3 K. Chuah, L. M. H. Lai, I. Y. Goon, S. G. Parker, R. Amal and J. Justin Gooding, *Chem. Commun.*, 2012, **48**, 3503–3505.

4 L. M. H. Lai, I. Y. Goon, K. Chuah, M. Lim, F. Braet, R. Amal and J. J. Gooding, *Angew. Chem. Int. Ed.*, 2012, **51**, 6456–6459.

5 L. M. H. Lai, I. Y. Goon, M. Lim, D. B. Hibbert, R. Amal and J. J. Gooding, *J. Electroanal. Chem.*, 2011, **656**, 130–135.